Chronology of CH···O Hydrogen Bonding from Molecular Dynamics Studies of the Phosphoric Acid-Catalyzed Allylboration of Benzaldehyde

Matthew N. Grayson,[†,∥] Zhongyue Yang,[‡,∥] and K. N. Houk*[,‡]

[†]Centre for Molecular Informatics, Department of Chemistry, University of Cambridge, Lensfield Road, Cambridge CB2 1EW, United Kingdom. [‡]Department of Chemistry and Biochemistry, University of California, Los Angeles, California 90095-1569, United States.

Supporting Information Placeholder

ABSTRACT: CH···O hydrogen bonds involving formyl groups have been invoked as a crucial factor controlling many asymmetric transformations. We have conducted quasi-classical direct molecular dynamics simulations on the phosphoric acid-catalyzed allylboration of benzaldehyde to understand the synergy between the phosphoric acid OH···O hydrogen bond and the secondary CH···O formyl hydrogen bond as the reaction occurs. In the gas phase, both the CH···O and OH···O hydrogen bonds are enhanced from reactants to transition states. In toluene, the trend of H-bond enhancement is observed with a smaller magnitude because of solvent caging. The strength of the formyl hydrogen bond in the TS, a second CH···O interaction between the P=O oxygen and *ortho*-hydrogen of the phenyl ring and the OH···O hydrogen bond were determined using quantum mechanical calculations (4.6, 1.0 and 14.5 kcal mol^{-1} respectively).

In a series of communications in 1997 and after, E. J. Corey proposed the importance of formyl CH···O hydrogen bonds for transition state stabilization in enantioselective asymmetric reactions.[1–5] This interaction was proposed based on X-ray crystal structures of aldehyde–Lewis acid complexes that contained formyl H to oxygen distances well within the sum of the van der Waals radii.[1] Since these pioneering studies, computational work has revealed that the formyl hydrogen bond plays a crucial role in many asymmetric transformations[6] including aldol,[7–9] allylboration,[10–11] aza-ene-type,[12] cycloaddition,[13] hydrohydroxyalkylation[14] and propargylation[15] reactions. X-ray crystallographic evidence has been debated, but seems in favor of the importance of CH···X interactions.[16]

Goodman and co-workers[10] found that Antilla's BINOL-derived phosphoric acid-catalyzed asymmetric allylboration of aldehydes[17] (**Scheme 1**) proceeds via a six-membered transition structure (TS) in which the Brønsted acidic site of the catalyst interacts with the pseudoaxial oxygen of the cyclic boronate and the P=O oxygen interacts with the formyl proton (TS Model, **Scheme 1**).

We have now conducted direct molecular dynamics (MD) simulations on this reaction to understand more about the timing and nature of this formyl hydrogen bond to O=P. Quantum mechanical calculations were also performed to provide an estimate of the strength of this interaction in the TS. The reaction of interest involves TRIP-PA catalysis of the allylboration of benzaldehyde shown in **Scheme 1**. For the computational studies, buta-1,3-diene-1,4-diol-phosphoric acid was used as a model for the full catalyst system (Model Catalyst, **Scheme 1**). Previous computational studies have shown that this truncated catalyst is a reliable model for BINOL-derived phosphoric acids.[10,15,18–22]

Scheme 1. Asymmetric Allylboration of Benzaldehyde.

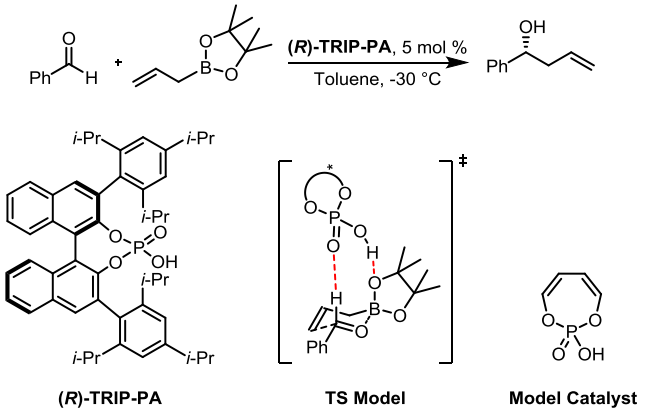

Direct molecular dynamics (MD) simulations were performed for the allylboration of benzaldehyde using our model catalyst (Scheme 1) in the gas phase and in toluene. We initialized 150 quasiclassical trajectories (QCTs) in the gas phase within the region of the potential energy surface near the transition structure (*supporting information*). Zero-point energy was added to each sampled TS for each real normal mode, along with a Boltzmann sampling of thermal energy available at 300 K with a random phase.[23,24] The trajectories were propagated forward and backward, for 150 fs in each direction. The classical equations of motion were integrated with a velocity-Verlet algorithm using Singleton's program Progdyn,[25] with the energies and derivatives computed on the fly by the B3LYP/6-31G(d) method using Gaussian 09. The step length for integration was 1 fs. When 150 QCTs were propagated in the gas phase, 142 of them were productive, and 8 recrossed.

For dynamics in toluene, solvent-perturbed transition state sampling protocol was applied.[26,27] Twenty-five solvent configurations were sampled with frozen TSs using classical MD. In each snapshot, the transition structure was optimized using the QM/MM method in Gaussian, with B3LYP/6-31G(d) applied for QM and GAFF for MM. Frequencies for each transition structure were calculated, and TS normal mode sampling was performed to obtain a Boltzmann distribution of TS geometries for dynamics.

This is defined as a solvent-perturbed transition state (SPTS), which is used to initialize trajectories in a solvent box.[26] Twenty-five QCTs were propagated in toluene with the B3LYP/6-31G(d)/GAFF method forward and backward for 150 fs in each direction. Twenty-two were productive, and three recrossed.

The strength of the formyl hydrogen bond (H-bond) was determined using quantum mechanical calculations performed with Gaussian 09 (Revision D.01).[28] All geometries were optimized using the B3LYP density functional,[29,30] and the 6-31G(d) basis set. Single point energies were calculated using M06-2X[31] and the polarized, triple-ζ valence quality def2-TZVPP basis set.[32] Computed structures were illustrated with CYLView.[33] To ensure that the B3LYP TS geometries were reliable, the allylboration of benzaldehyde TS was reoptimized using M06-2X. Superposition of the six reacting ring atoms and the catalyst phosphorous atom in these TSs allowed calculation of an RMSD value of 0.09 Å, suggesting minimal geometric change between the 2 TSs.

Direct dynamics simulations were conducted to study the timing of changes in H-bonding, that we call the chronology of the benzaldehyde formyl H-bond to O=P (CH···O) and the phosphoric acid hydrogen bond to the boronate O (OH···O) in the gas phase and in toluene. **Figure 1a** shows the snapshots of a typical productive trajectory in the gas phase. The phosphoric acid catalyst stabilizes the transition state by H-bonding to the boronate O. The boronate ester becomes partially negative in the TS as the aldehyde O forms a bond to B. The boronate O becomes a good H-bond acceptor. At the same time, the formyl group becomes more positive and becomes a CH H-bond donor. For this trajectory, the length of the CH···O distance is 3.0 Å at -150 fs (hardly an H-bond at all), 2.1 Å at 0 fs, and 2.3 Å at 150 fs. In comparison, the length of the OH···O H-bond is 1.9 Å at -150 fs, 1.6 Å at 0 fs, and 2.1 Å at 150 fs. From -150 fs to 0 fs, the CH···O H-bond decreases by 0.9 Å, and the OH···O H-bond decreases by 0.3 Å. This indicates that both hydrogen bonds are enhanced in the transition state. **Figure 1b** displays the snapshots for a typical productive trajectory in toluene. The length of the CH···O H-bond is 2.3 Å at -150 fs, 2.1 Å at 0 fs and 2.5 Å at 150 fs, while that of the OH···O H-bond is 1.7 Å at -150 fs, 1.6 Å at 0 fs, and 2.2 Å at 150 fs. A smaller magnitude of enhancement is observed relative to the gas phase, which is likely caused by the solvent caging effect of toluene molecules.

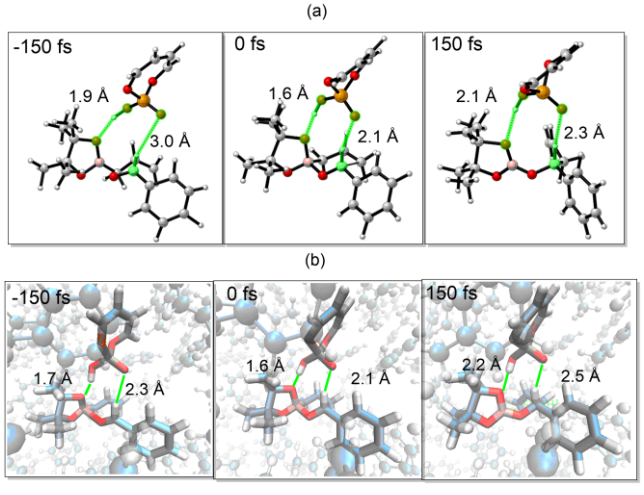

Figure 1. Snapshots for typical reactive trajectories in the catalyzed allylboration of benzaldehyde (a) in the gas phase, and (b) in toluene.

The statistics of the CH···O and OH···O distances in the gas phase are shown in **Figure 2a** and **2b**, respectively. In each trajectory, the geometries at -150 fs, 0 fs, and 150 fs are defined as reactant, transition state and product, respectively. **Figure 2a** shows that in the gas phase, the distribution of the CH···O distances in the transition states range from 1.8 Å to 2.8 Å, which is about half as narrow as that in the reactant or products (from 1.8 Å to 3.5 Å). Here we define the H-bond cutoff as 2.25 Å.[34] The percentage of trajectories possessing a CH···O H-bond is 8% in reactants, 53% in transition states, and 5% in products. This shows a significant increase in the percentage of CH···O H-bonds from reactant to transition state. **Figure 2b** shows that the OH···O H-bond lengths of the transition state range from 1.3 Å to 2.0 Å, which is also about half as narrow as that in reactants or products (from 1.3 Å to 3.0 Å). The percentage of trajectories involving H-bond is 95% in reactants, 100% in transition states, and 70% in products. This indicates that the OH···O H-bond is formed in most trajectories from reactant to the TS. The average distance of the OH···O H-bond is 1.9 Å for reactants, 1.6 Å for transition states, and 2.2 Å for products. This indicates an enhancement of the OH···O H-bond from reactant to the TS.

(a) CH···O Hydrogen Bond

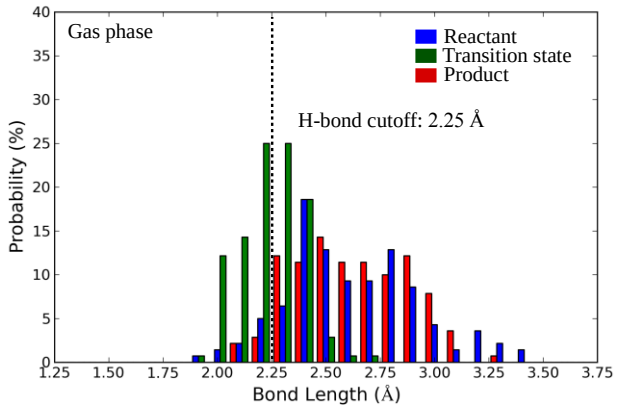

(b) OH···O Hydrogen Bond

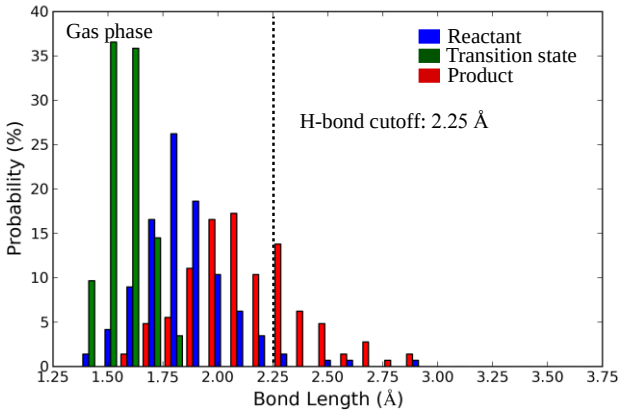

Figure 2. Distribution of (a) benzaldehyde formyl hydrogen bond (CH···O) distances and (b) phosphoric acid hydrogen bond (OH···O) distances in the gas phase at reactants, transition states, and products. In each trajectory, the transition state is at 0 fs, and the reactants and products are defined as structures at -150 fs, and 150 fs, respectively. H-bond cutoff is set as 2.25 Å.

As shown in **Figure 3**, in toluene, the percentage of trajectories possessing a CH···O H-bond is 28% in reactants, 50% in the TS, and 8% in products, while the average distance of the OH···O H-bond lengths is 1.7 Å for reactants, 1.5 Å for transition states, and 1.9 Å for products. The enhancements of both CH···O and OH···O hydrogen bonds are also observed in toluene, even though with a smaller magnitude for the CH···O H-bond.

(a) CH···O Hydrogen Bond

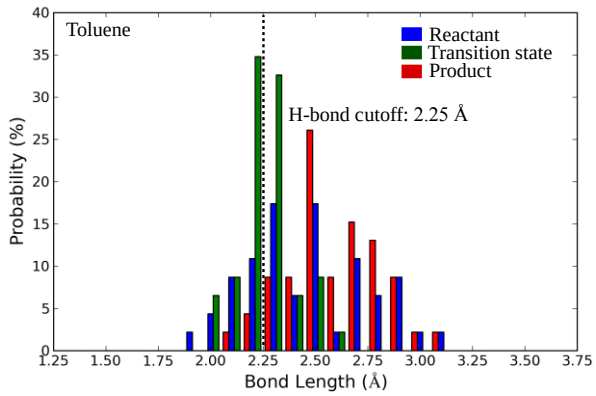

(b) OH···O Hydrogen Bond

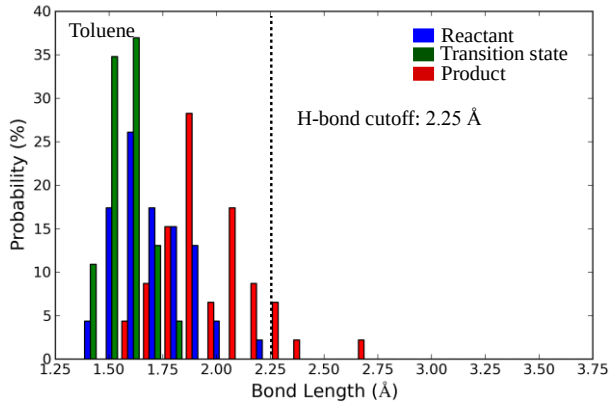

Figure 3. Distribution of (a) benzaldehyde formyl hydrogen bond (CH···O) distances and (b) phosphoric acid hydrogen bond (OH···O) distances in toluene at reactants, transition states, and products. In each trajectory, the transition state is at 0 fs, and the reactants and products are defined as structures at -150 fs, and 150 fs, respectively. H-bond cutoff is set as 2.25 Å.

Figure 4 shows the average of CH···O and OH···O distances versus time. Both bond lengths decrease from reactant to transition state, and then increase until the formation of products. This indicates the enhancement of both hydrogen bonds during the allylboration of benzaldehyde. This synergy results from a partial charge separation as the B-O bond forms between the allylboronate and benzaldehyde in the transition state. The charge separation increase the acidity of the benzaldehyde hydrogen and the basicity of the allylboronate oxygen. This reinforces the formation of both CH···O and OH···O hydrogen bonds. The charge separation decreases, however, as the product forms, which is accompanied by a change of the hybridization state of the carbonyl carbon from sp^2 to sp^3. This causes the decline in both hydrogen bond lengths from TS to product. Other possibilities, such as statistical fluctuation and entropic effects, were excluded as reasons for the observed bond length decrease (see supporting information, page S9).

We also investigated the difference between the averaged dynamics motion and the IRC in the supporting information, page S10. Singleton recently pointed out that the difference between hydrogen and heavy atoms results in their different time scales of motion.[35] This makes the dynamical behaviors of trajectories sometimes deviate from what IRC would expect. Our results show that the IRC does not reveal the enhancement of hydrogen bonds during the reaction course, but trajectories do. This highlights the importance of time-resolved studies in the elucidation of reaction mechanisms.

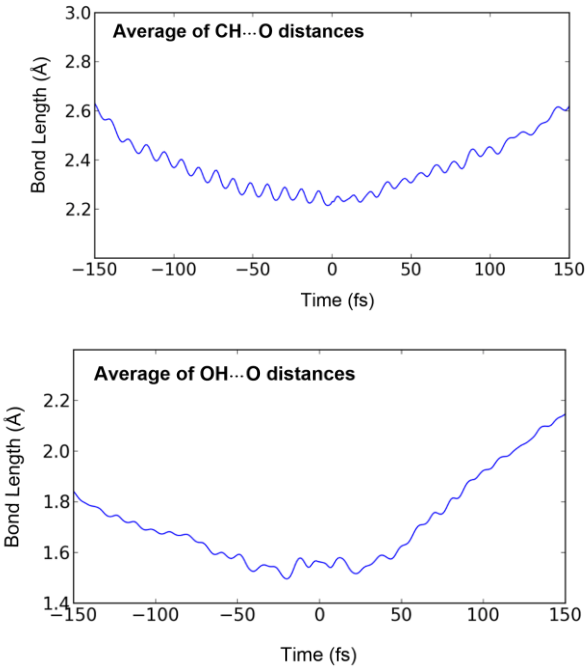

Figure 4. Dynamics of averaged CH···O and OH···O distances in the gas phase. One hundred and forty two product trajectories were averaged.

CH···O H-bond is a weak interaction that might be dynamically affected by neighboring solvent molecules. Consequently, we investigated the evolution of CH···O H-bond from reactant to the transition state for trajectories in the gas phase and in toluene. As shown in **Figure 5**, in the gas phase, the percentage of trajectories possessing CH···O H-bond is low (8%), and keeps increasing until it reaches the maximum (53 %) around the transition state. In contrast, for trajectories in toluene, the percentage fluctuates between 28% and 50% from reactant to transition state. This suggests that toluene molecules favor the formation of CH···O H-bond in reactant by keeping two reacting molecules in one solvent cage, but detracts from H-bonding in the TS. Our results only provide a qualitative understanding because of the limited number of trajectories in toluene.

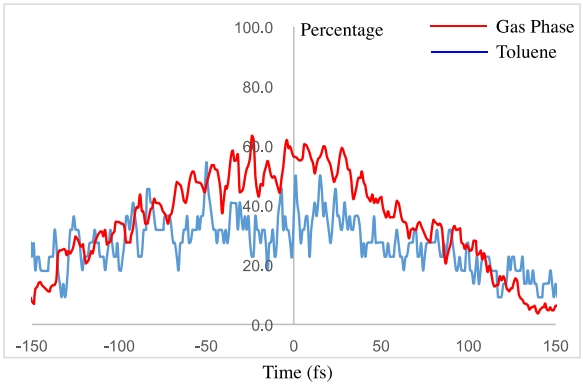

Figure 5. Evolution of percentage of trajectories possessing CH···O hydrogen bonds in the gas phase and in toluene. The H-bond criteria is defined as 2.25 Å.

To provide an estimate of the strength of the formyl hydrogen bond in the TS, quantum mechanical calculations were also performed (**Figure 6**). Allylboronic acid pinacol ester was removed from the gas phase TS, **TS-1**, and without further optimization, the energy of the catalyst-aldehyde complex was evaluated. This energy value was compared to the sum of the energy of the individual unoptimized fragments to determine the interaction energy

between them (5.6 kcal mol^{-1}, **Figure 6**). However, the P=O of the catalyst also interacts with the *ortho*-hydrogen of the phenyl ring. **TS-2** (aldehyde = ethanal) was located in which the *ortho*-hydrogen interaction was absent and, using the same process as outlined above, the interaction energy was calculated to be 4.6 kcal mol^{-1} (**Figure 6**). Therefore, the strength of the formyl hydrogen bond and the second CH···O interaction are approximately 4.6 and 1.0 kcal mol^{-1} respectively. The OH···O hydrogen bond strength was estimated to be 14.5 kcal mol^{-1} by measuring the interaction energy between the allylboronic acid pinacol ester and model phosphoric acid catalyst in **TS-1**.

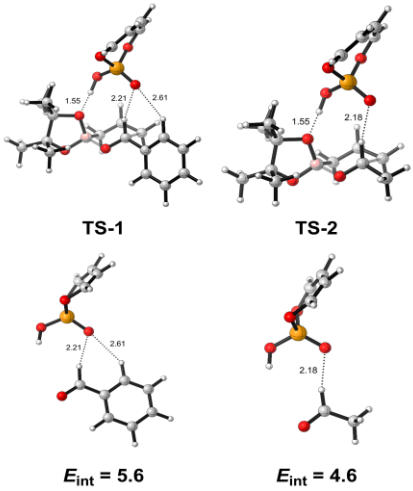

Figure 6. Catalyst-aldehyde interaction energies for **TS-1** (aldehyde = benzaldehyde) and **TS-2** (aldehyde = ethanal). M06-2X/def2-TZVPP//B3LYP/6-31G(d). All energies in kcal mol^{-1}.

Molecular dynamics simulations on the phosphoric acid-catalyzed allylboration of benzaldehyde have shown that in the gas phase and toluene, a synergy between the enhancement of both the formyl hydrogen bond (CH···O) and the phosphoric acid hydrogen bond (OH···O) occurs in the TS relative to the reactants. Toluene molecules favor the formation of the CH···O H-bond in the reactant by keeping two reacting molecules in one solvent cage, but diminish the further enhancement of CH···O H-bonds in the TS. The strengths of the formyl hydrogen bond in the TS, and of the CH···O interaction between the P=O oxygen and *ortho*-hydrogen of the phenyl ring and the OH···O hydrogen bond were determined using quantum mechanical calculations and were found to be 4.6, 1.0, and 14.5 kcal mol^{-1}, respectively.

ASSOCIATED CONTENT

Supporting Information

Computational details and data and complete Gaussian 09 reference.

AUTHOR INFORMATION

Corresponding Author

houk@chem.ucla.edu

Author Contributions

‖M.N.G. and Z. Y. contributed equally.

Notes

The authors declare no competing financial interests.

According to the University of Cambridge data management policy, all the data used in this paper is available either in the paper or in the Supporting Information.

ACKNOWLEDGMENT

We are grateful to The English-Speaking Union (Lindemann Trust Fellowship to M.N.G.), Girton College, Cambridge (Research Fellowship to M.N.G.) and the NSF (CHE-1361104 to K.N.H.) for financial support. Computational resources were provided by the UCLA Institute for Digital Research and Education (IDRE) and the Extreme Science and Engineering Discovery Environment (XSEDE), which is supported by the NSF (OCI-1053575).

REFERENCES

(1) Corey, E. .; Rohde, J. J.; Fischer, A.; Azimioara, M. D. *Tetrahedron Lett.* **1997**, *38*, 33–36.
(2) Corey, E. J.; Rohde, J. J. *Tetrahedron Lett.* **1997**, *38*, 37–40.
(3) Corey, E. J.; Barnes-Seeman, D.; Lee, T. W. *Tetrahedron Lett.* **1997**, *38*, 1699–1702.
(4) Corey, E. J.; Barnes-Seeman, D.; Lee, T. W. *Tetrahedron Lett.* **1997**, *38*, 4351–4354.
(5) Corey, E. J.; Lee, T. W. *Chem. Commun.* **2001**, 1321–1329.
(6) Johnston, R. C.; Cheong, P. H.-Y. *Org. Biomol. Chem.* **2013**, *11*, 5057–5064.
(7) Paton, R. S.; Goodman, J. M. *Org. Lett.* **2006**, *8*, 4299–4302.
(8) Paton, R. S.; Goodman, J. M. *J. Org. Chem.* **2008**, *73*, 1253–1263.
(9) Yang, H.; Mahapatra, S.; Cheong, P. H. Y.; Carter, R. G. *J. Org. Chem.* **2010**, *75*, 7279–7290.
(10) Grayson, M. N.; Pellegrinet, S. C.; Goodman, J. M. *J. Am. Chem. Soc.* **2012**, *134*, 2716–2722.
(11) Rodríguez, E.; Grayson, M. N.; Asensio, A.; Barrio, P.; Houk, K. N.; Fustero, S. *ACS Catal.* **2016**, *6*, 2506–2514.
(12) Terada, M.; Soga, K.; Momiyama, N. *Angew. Chem. Int. Ed.* **2008**, *47*, 4122–4125.
(13) Paddon-Row, M. N.; Anderson, C. D.; Houk, K. N. *J. Org. Chem.* **2009**, *74*, 861–868.
(14) Grayson, M. N.; Krische, M. J.; Houk, K. N. *J. Am. Chem. Soc.* **2015**, *137*, 8838–8850.
(15) Grayson, M. N.; Goodman, J. M. *J. Am. Chem. Soc.* **2013**, *135*, 6142–6148.
(16) Taylor, R.; Kennard, O. *J. Am. Chem. Soc.* **1982**, *104*, 5063–5070.
(17) Jain, P.; Antilla, J. C. *J. Am. Chem. Soc.* **2010**, *132*, 11884–11886.
(18) Simón, L.; Goodman, J. M. *J. Am. Chem. Soc.* **2008**, *130*, 8741–8747.
(19) Simón, L.; Goodman, J. M. *J. Am. Chem. Soc.* **2009**, *131*, 4070–4077.
(20) Simón, L.; Goodman, J. M. *J. Org. Chem.* **2010**, *75*, 589–597.
(21) Simón, L.; Goodman, J. M. *J. Org. Chem.* **2011**, *76*, 1775–1788.
(22) Overvoorde, L. M.; Grayson, M. N.; Luo, Y.; Goodman, J. M. *J. Org. Chem.* **2015**, *80*, 2634–2640.
(23) Chapman, S.; Bunker, D. L. *J. Chem. Phys.* **1975**, *62*, 2890–2899.
(24) Doubleday, C. E.; Bolton, K.; Hase, W. L. *J. Phys. Chem. A* **1998**, *102*, 3648–3658.
(25) Wang, Z.; Hirschi, J. S.; Singleton, D. A. *Angew. Chem. Int. Ed.* **2009**, *48*, 9156–9159.
(26) Yang, Z.; Doubleday, C.; Houk, K. N. *J. Chem. Theory Comput.* **2015**, *11*, 5606–5612.
(27) Liu, F.; Yang, Z.; Mei, Y.; Houk, K. N. *J. Phys. Chem. B* **2016**, *120*, 6250–6254.
(28) Frisch, M. J., et al. Gaussian 09; Gaussian, Inc., Wallingford, CT, 2013.
(29) Becke, A. D. *Phys. Rev. A* **1988**, *38*, 3098–3100.
(30) Lee, C.; Yang, W.; Parr, R. G. *Phys. Rev. B* **1988**, *37*, 785–789.
(31) Zhao, Y.; Truhlar, D. *Theor. Chem. Acc.* **2008**, *120*, 215–241.
(32) Weigend, F.; Ahlrichs, R. *Phys. Chem. Chem. Phys.* **2005**, *7*, 3297–3305.

(33) Legault, C. Y. CYLView, 1.0b; Université de Sherbrooke: Sherbrooke, Quebec, Canada, 2009; http://www.cylview.org.
(34) Desiraju, G. R. *Acc. Chem. Res.* **1996**, *29*, 441-449.
(35) Aziz, D. A.; Singleton, D. A. *J. Am. Chem. Soc*. **2017**, *139*, 5965–5972.